



**HAL**  
open science

## Surface properties assessment of reclaimed carbon fibres for recycling in PA6/CF composites

Louis Jeantet, Arnaud Regazzi, Perrin Didier, Monica Francesca Pucci,  
Stéphane Corn, Jean-Christophe Quantin, Patrick Ienny

### ► To cite this version:

Louis Jeantet, Arnaud Regazzi, Perrin Didier, Monica Francesca Pucci, Stéphane Corn, et al.. Surface properties assessment of reclaimed carbon fibres for recycling in PA6/CF composites. ICCM 23 - 23rd International Conference on Composites Materials, Queen's University Belfast, Jul 2023, Belfast (Northern Ireland), United Kingdom. hal-04186058

**HAL Id: hal-04186058**

**<https://hal.science/hal-04186058>**

Submitted on 13 Nov 2023

**HAL** is a multi-disciplinary open access archive for the deposit and dissemination of scientific research documents, whether they are published or not. The documents may come from teaching and research institutions in France or abroad, or from public or private research centers.

L'archive ouverte pluridisciplinaire **HAL**, est destinée au dépôt et à la diffusion de documents scientifiques de niveau recherche, publiés ou non, émanant des établissements d'enseignement et de recherche français ou étrangers, des laboratoires publics ou privés.

# SURFACE PROPERTIES ASSESSMENT OF RECLAIMED CARBON FIBRES FOR RECYCLING IN PA6/CF COMPOSITES

L. JEANTET<sup>1,2</sup>, A. REGAZZI<sup>2\*</sup>, D. PERRIN<sup>3</sup>, M.F. PUCCI<sup>2</sup>, S. CORN<sup>2</sup>, J.-C. QUANTIN<sup>2</sup>, P. IENNY<sup>2</sup>

<sup>1</sup> Segula Technologies, 19 rue d'Arras, Nanterre 92000, France

<sup>2</sup> LMGC, IMT Mines Ales, Univ Montpellier, CNRS, Ales, France

<sup>3</sup> Polymers composites and hybrids (PCH), IMT Mines Ales, France

**Keywords:** Recycling, Carbon Fibre, Interfacial shear strength

## ABSTRACT

Carbon fibre reclaiming and reuse is both an environmentally and economically fruitful endeavour. The reuse of pyrolysis reclaimed carbon fibres (RCF) in meaningful quantities for high performance parts is promising. However, the harmfulness of the reclaiming process to the mechanical properties of fibres and their adhesion capabilities with polymeric matrix must be investigated. This paper studies the mechanical and surface properties of pyrolysis RCF in comparison with sized and de-sized fibres to assess their potential for reuse. Tensile mechanical properties of these three fibre types were evaluated via micromechanical tensile testing of single fibre samples. RCF show a minor diminution in tensile strength and unchanged elastic modulus which makes these intrinsic mechanical properties suitable for reuse in composite parts. The morphology of the fibre surfaces were analysed using scanning electron microscopy and atomic force microscopy. The scans show clearly different morphologies. RCF present polymeric residues as well as smooth areas very similar to de-sized fibres. Atomic force microscopy was also used to measure the roughness of fibre surfaces. The mean roughness of RCF surfaces was higher than that of de-sized fibres but lower than that of sized fibres. In that context, the residual polymer might be a contributor to better interfacial properties between the fibre and the matrix. Tensiometric tests were carried out to determine fibre surface energy. The RCF showed higher surface energies than de-sized fibres suggesting better adhesion. However, this finding did not transfer to better cohesion between RCF and the polymer matrix. Indeed, in IFSS testing both RCF and de-sized fibres showed similar interfacial shear strength values. The outcomes of this work contribute to the optimisation of the reclaimed carbon fibre re-use in composites. In particular, they highlight the necessity for a surface treatment on RCF to enhance fibre/matrix adhesion and thus composite mechanical properties.

## 1 INTRODUCTION

Carbon fibre reinforced polymer (CFRP) composites have become in recent years a staple material in high performance industries such as aircraft manufacturing and automotive [1,2]. Their high tensile strength and lightweight properties are highly useful in those endeavours. The newfound abundance of these materials has created a need for a more sustainable production and a controlled life cycle. Reclaiming carbon fibre from composite waste has been established as economically and environmentally beneficial.

The carbon balance of the reclaiming process is positive, even for energy demanding processes such as pyrolysis, as the energy demands for the carbon fibre (CF) manufacturing process are tremendous [3,4]. As a result, reclaiming processes that can be scaled to industrial proportions, such as pyrolysis reclaiming, have been developed and are used to process composite waste [5]. With the

increasing use of CFRP in airplane carriers, there is an endless supply of composite waste to repurpose and, at the same time, an increased demand for high performance composite parts.

However, the nature of the recycling process does not allow for reuse of the reclaimed fibres (RCF) in woven CF fabric, for the time being. To reuse the RCF in high performance application, the recycled composite formulation will need to be optimized for cut random fibres. Moreover, previous studies highlight that, although the reclaiming process does not affect the fibre intrinsic mechanical properties significantly, it does negatively affect the polymer/fibre interfacial properties [6,7]. This phenomenon then translates to lower composite mechanical properties as the interface between the components of the composite materials is impaired in comparison with a composite produced using sized virgin CF. This effect could be due to a degraded fibre surface chemical state, less mechanical interlocking via surface roughness modification, or both.

The aim of this study is to determine and quantify the factors that influence the interfacial properties of the pyrolysis RCF. This will then allow the selection of a specific restorative treatment to grant optimal cohesion between the RCF and the matrix. As a result, competitive mechanical properties of the recycled composite material will be ensured. The intrinsic mechanical properties of the RCF were evaluated via micromechanical testing to ensure no significant change in mechanical properties compared to virgin fibres (VF) would interfere with further experiments. The modifications of the wettability of fibres surface by the reclaiming process were characterized via single fibre contact angle determination. The RCF surface morphology and roughness were evaluated using scanning electron microscopy and atomic force microscopy. The fibre/matrix interfacial shear strength (IFSS) was then assessed from microdroplet tests.

## 2 MATERIALS

The thermoplastic matrix selected for the preparation of composites was Technyl C206F Natural, a commercially available PA6 produced by Solvay (Brussels, Belgium). Sized virgin fibres of different origins obtained from spools of pure carbon fibres with a PA6 sizing and cut to a length of 20 mm were supplied by Procotex (Mouscron, Belgium). Reclaimed carbon fibres were purchased from ELG Carbon Fibre (Bilston, United Kingdom), the fibres were cut to a 20 mm mean length after a two-step reclaiming process. According to previous studies using these fibres [8,9], the two-step treatment consists of a pyrolysis treatment of 30 min at 500 °C under nitrogen followed by a second step of thermo-oxidation of 10 min at 500 °C under air to remove the char produced during pyrolysis. A third type of fibre was prepared by making the virgin fibres undergo a thermo-oxidative treatment, like the char-removing treatment used by ELG (i.e. 10 min at 500 °C under air), to eliminate the coating. For clarity purposes virgin fibres will be noted as VF, commercial reclaimed fibres will be referred to as RCF and virgin fibres after thermal treatment as VFT.

## 3 METHODS

### 3.1 Fibres tensile testing

Fibre transverse dimensions were determined using a FDAS770 fibre dimensional analysis system from Dia-Stron (Andover, UK). 200 projections of the rotating fibre were acquired at 20 locations along its length to determine local minimum and maximum diameters  $D_{min}$  and  $D_{max}$  respectively. The corresponding cross-sectional areas were computed assuming that each cross-section is elliptical.

Fibre mechanical properties were evaluated using a LEX820 linear extensometer from Dia-Stron. Tensile stress at break was calculated using the following equation:

$$\sigma = \frac{F}{S_{mean}} \quad (1)$$

Where  $F$  is the force at break, and  $S_{mean}$  being the mean value of the elliptical cross-sectional areas of the fibre. Displacement values measured during tensile testing were adjusted to consider the inherent compliance of the experimental set-up according to the ISO 11566:1996(EN) standard. The compliance

value was established at  $0.28 \text{ mm.N}^{-1}$  for our device (from a preliminary assessment performed on similar samples with various lengths). For each fibre type, the repeatability was ensured by testing 25 samples. The nominal fibre length of these samples was 12 mm. Tensile modulus was determined by linear regression of the stress vs strain plots, in the elastic deformation domain between 0.05 % and 0.25 % deformation according to the ISO 11566:1996(EN) standard..

### 3.2 Scanning Electron Microscopy and fibre morphology assessment

A Quanta 200 FEG scanning electron microscope (SEM) from FEI Company (Hillsboro, USA) operating at 4 kV was used to observe the surface morphology of the fibres.

### 3.3 Atomic Force Microscopy fibre topography and fibre roughness determination

An MFP-3D Infinity atomic force microscope (AFM) from Asylum Research (Santa Barbara, USA) was used in a tapping mode to assess the topography of fibres. From this topographic data, roughness values were computed. Single fibres were fixed to a glass slide for tests. A silicon probe (AC160TS-R3) with a resonant frequency of 300 kHz and a spring constant of 25 N/m was used. The scan rate was set to 1 Hz. Topography images with a region of interest (ROI) of  $3 \times 3 \mu\text{m}^2$  were obtained at a resolution of  $256 \times 256$  pixels. A three-dimensional topography of the fibre's surface was acquired using the IGOR Pro 6.27 software. These scans were then processed using a Matlab program to deduce the roughness values by subtracting the natural curvature of the fibre surfaces. According to the ISO 21920-2:2021 standard, the reported roughness values use the common statistical descriptor  $S_q$  (height root mean square) expressed as:

$$S_q = \sqrt{\frac{1}{A} \iint_A dz^2(x, y) dx dy} \quad (2)$$

Where  $A$  is the area of the ROI and  $z(x, y)$  a function giving the height value for a given data point defined by its abscissa  $x$  and its ordinate  $y$ .

### 3.4 Fibres wettability evaluation

3.1 Contact angle tests on single fibres were performed using a Krüss K100 tensiometer at ambient temperature using the Wilhelmy principle [10]. Test liquids used were n-hexane, water, diiodomethane and ethylene glycol. Water was used for its high polarity and surface tension, n-hexane was used as a totally wetting liquid, due to its low surface tension, diiodomethane was used for its low polarity while not totally dispersive, and the ethylene glycol was used for its good balance between the two components. The vessel speed was  $1 \text{ mm.min}^{-1}$  and the immersion length 3 mm. The Wilhelmy relationship was used to determine the contact angles:

$$F_c = P \gamma_l \cos \theta \quad (3)$$

Where  $F_c$  is the capillary force measured by the tensiometer,  $\gamma_l$  is the surface energy of the test liquid,  $\theta$  is the measured contact angle, and  $P$  is the perimeter of the fibre. Perimeter of fibre was obtained thanks to tests described in section 3.1. The advancing and receding contact angles were measured as well, only the static angle was considered for the surface energy assessment. Contact angles presented here were determined from a mean of at least 7 contact angles measurements. Surface energies of fibres were deduced from these values using the Owens-Wendt relation in a linear representation:

$$\frac{\gamma_l(1+\cos\theta)}{2\sqrt{\gamma_l^d}} = \sqrt{\gamma_s^p} \frac{\sqrt{\gamma_l^p}}{\sqrt{\gamma_l^d}} + \sqrt{\gamma_s^d} \quad (4)$$

With the polar and dispersive components of test liquids ( $\gamma_l^d$  and  $\gamma_l^p$ ) and equilibrium known contact angles, this equation allows the determination of the polar and dispersive components of solid surface energy of the fibre surfaces ( $\gamma_s^d$  and  $\gamma_s^p$ ).

### 3.5 Microdroplet IFSS testing

The samples were prepared in a similar manner as described by Ma et al. [11]. Finely ground PA6 was obtained by cryogenic grinding of the pellets. This powder was then applied to the fibre using electrostatic adhesion and heated to 240 °C using a copper wire. An example of a sample is presented in Figure 1.

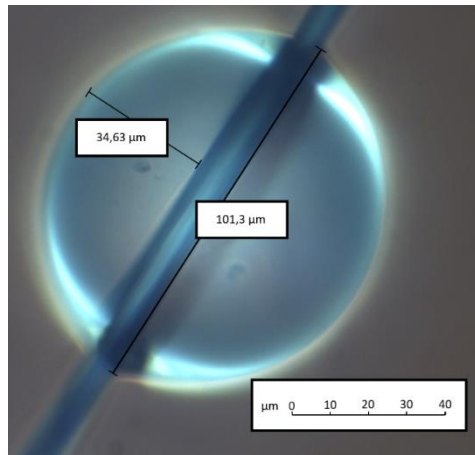


**Figure 1 – Microdroplet sample observed via optical microscopy**

The melted polymer then naturally formed microdroplets around the fibre. Adequately sized droplets were selected using an optical microscope equipped with a camera to measure their diameter and embedded length. The droplets were selected to have an embedded length between 60 and 120  $\mu\text{m}$ . Mechanical characterization of the fibre/matrix system was conducted using a LEX820 linear extensometer from Dia-Stron equipped with the microdroplet pull-out module and a 20  $\mu\text{m}$  vise. The droplet was positioned at a 500  $\mu\text{m}$  distance from the vise and then pulled over 800  $\mu\text{m}$  through it using a 5  $\mu\text{m}\cdot\text{s}^{-1}$  testing speed. The contact of the droplet with the vise created an increase in the measured charge that ended with the detachment of the droplet. The peak force value at debonding  $F_p$ , is then used to determine the IFSS value, using the equation:

$$IFSS = \frac{F_p}{\pi L(3(D_{min}+D_{max})-\sqrt{(3D_{min}+D_{max})(D_{min}+3D_{max})})} \quad (5)$$

Where  $L$  is the measured embedded length for each fibre, and  $D_{min}$  and  $D_{max}$  are mean values determined for each fibre type using the FDAS770 fibre dimensional analysis system from Dia-Stron.

Cross-sections of the fibres were considered elliptical, and their perimeter was approximated using the Ramanujan formula [12].

## 4 RESULTS AND DISCUSSION

### 4.1 Fibres mechanical properties

The mean tensile strength of the single fibre CF samples is presented for each fibre type in Figure 2. As expected, RCF shows a tensile strength 15 % inferior compared to the other two fibre types. These values agree with the mechanical performance reported by the supplier as well as the literature on pyrolysis RCF [13,14].

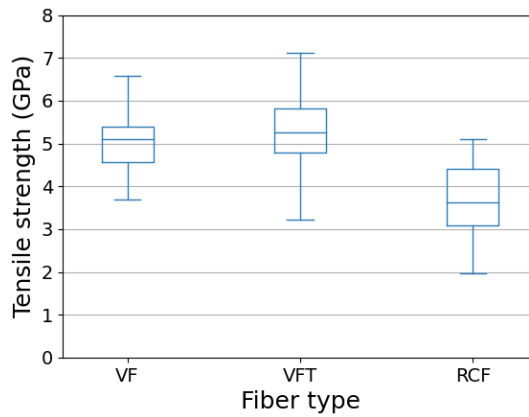


Figure 2 – Tensile strength mean values for each fibre type

The mean tensile strength values of the two other types of fibre, VFT and VF, are not significantly different. This suggests that the short (10 min) thermo-oxidative treatment used to remove the char from the surface of the VF does not negatively affect their mechanical properties. Long exposure to high temperatures (around 500 °C) however seems to cause a mild diminution of the tensile strength of the fibres. The diminution of the fibre mass and diameter, leading to a higher concentration of fracture inducing defects in a given volume, is the preferred hypothesis to explain this phenomenon in the literature [15].

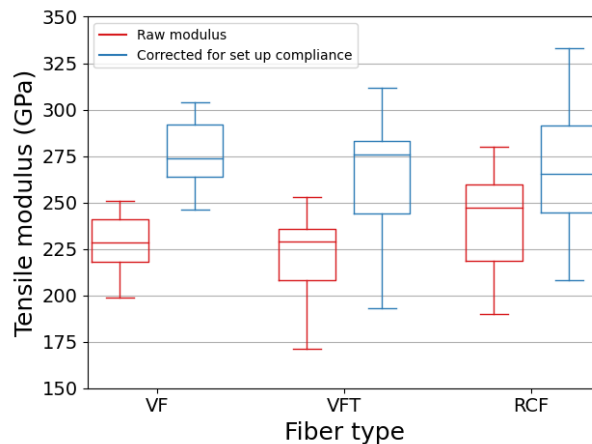


Figure 3 – Tensile modulus values calculated using raw displacement output and corrected for system compliance

In contrast, the three fibre types have very similar tensile moduli, as shown in Figure 3. The main difference is the dispersion of the data, with the VFT and RCF having a larger standard deviation compared to VF. Combined to the diminution in tensile strength, these results indicate that the recycling process increases the probability of rupture of the fibre by increasing the incidence of defects. On the other hand, elastic properties are unaffected by these changes.

#### 4.2 Fibre surface morphology

SEM observations of the three fibre types are illustrated in

Figure 4. The textures of the different samples show clear differences. RCF have a smooth surface with localized aggregations of residual polymer that resisted the reclaiming process. VFT have a very similar smooth surface all around without the chunks of residual polymer, the sizing seems to have been entirely removed revealing the bare fibre surface. VF have a more textured appearance showing the presence of sizing, dark spots are dispersed on the surface demonstrating that the sizing is heterogeneously distributed on the fibre.

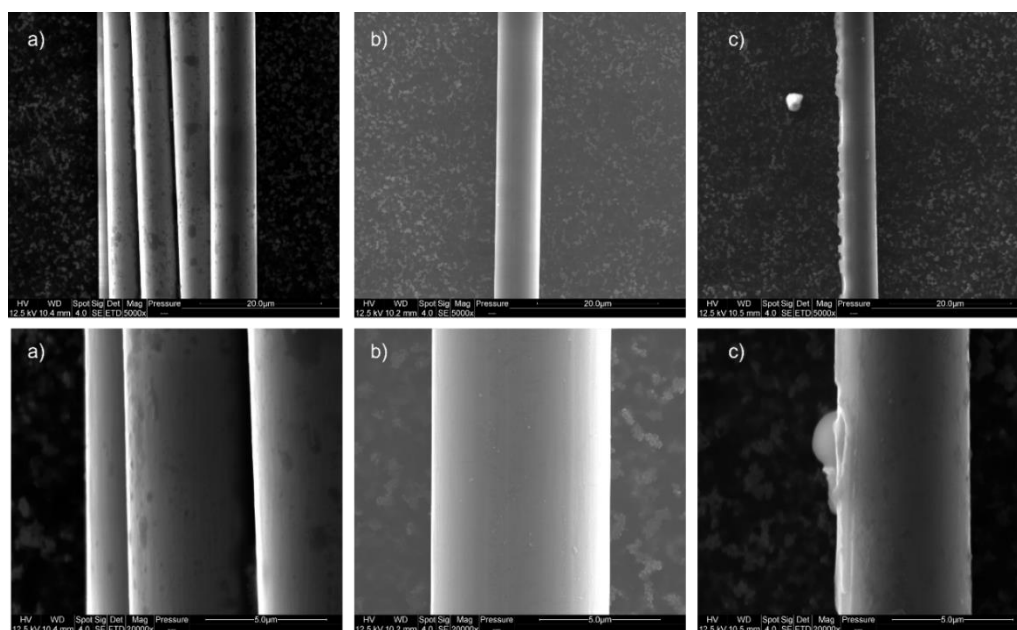


**Figure 4 – SEM scan of a) bundle of VF, b) VFT, c) RCF**

These SEM images show clear morphological differences between the surfaces of the three fibre types. In order to quantify the differences of fibre morphology, fibre surface roughness would need to be determined. That is why topography must be assessed by AFM to quantify the roughness values of the fibres surfaces.

#### 4.3 Fibre surfaces topography

AFM scans of RCF, VFT and VF are illustrated in Figure 5. An additional scan of RCF showing a smooth portion of the fibre surface, without the presence of residual polymer, was also acquired. The surface of RCF shows a very heterogeneous surface with chunks of residual polymer as well as smoother areas. In the case of the sample without residual polymer, the fibre bare surface is exposed with a very smooth and homogenous surface aspect. In a similar fashion, VFT surface is very smooth and

homogeneous without residual polymer nor sizing. In contrast, VF has a visually grainy appearance which suggests a high roughness due to the sizing heterogeneous repartition.

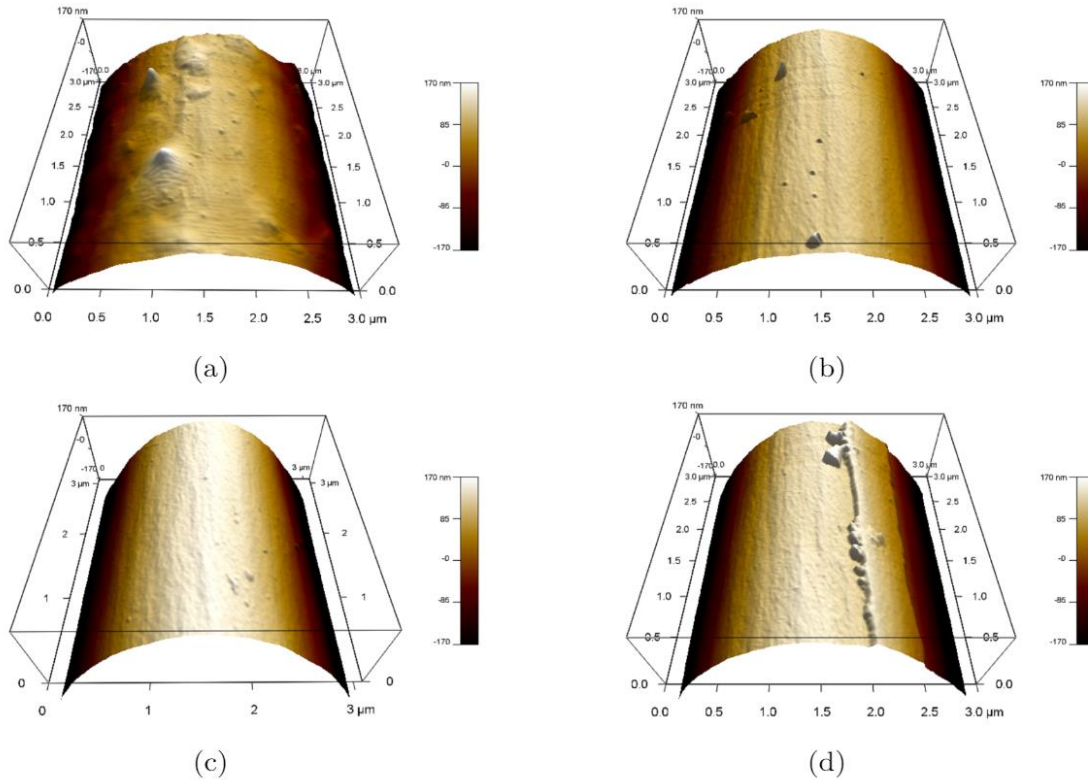


**Figure 5 - Topography of a  $3 \times 3 \mu\text{m}$  ROI of a) VF, b) VFT, c) smooth RCF, d) rough RCF**

The overall appearance of the samples is consistent with previous SEM observations. The results are shown in Table 1.

	$Sq$ [nm]	Highest peak [nm]	Deepest pit [nm]
VF	23	154.4	-53.9
VFT	5.6	43	-26.8
RCF (rough)	9.3	45.3	-31.9
RCF (smooth)	3.4	27.4	-13.1

**Table 1 – Roughness measurement for each fibre type**

The VF has the highest roughness, that should facilitate the mechanical interlocking with the matrix. VFT and smooth RCF have low roughness, probably due to the removal of sizing. RCF with polymeric residues has higher mean roughness because of localized polymeric residues. Higher roughness could play a favourable role on mechanical interlocking and then on fibre/matrix cohesion. Cohesion will be characterised thanks to IFSS microdroplet testing.



#### 4.4 Fibre surface wettability

Surface energies and components were determined to evaluate the potential adhesion of the fibre with the matrix. Values obtained for each fibre type are displayed in Figure 6. In previous studies [16,17], the main predictors of the adhesion of fibres to polymer matrix were the total surface energy and the ratio of polar component over said total energy. These two factors are, respectively, 0.63 and 39.9 mN/m for VF; 0.52 and 36.2 mN/m for VFT, 0.58 and 38.9 mN/m for RCF. Despite the absence of sizing, RCF still has a relatively high surface energy ratio thanks to the presence of polymeric matrix residues, which affects the wettability of fibres surface. Based on surface energies, RCF exhibits a better potential for adhesion to a polymeric matrix than VFT. This is due to the residual polymer not eliminated by the recycling process allowing for better chemical bonding.

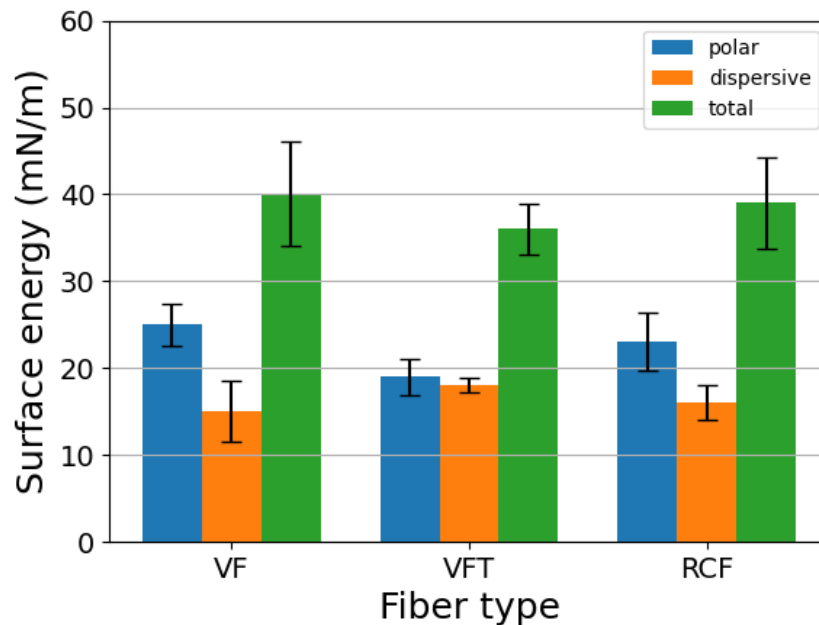


**Figure 6 - Surface energy values for each fibre type**

As expected, the sizing present on VF surfaces generates the highest values of surface energies that improve the adhesion with the thermoplastic matrix. The improvement in adhesion properties is correlated in the literature with increased interfacial shear strength. This has to be confirmed experimentally through IFSS testing.

#### 4.5 Interfacial shear strength

The interfacial shear strength values obtained from microdroplets pull-out tests are shown in Figure 7. The interfacial shear strength between PA6 and VF is about 40 % higher than with VFT or RCF. These results confirm that, in the case of short CF and thermoplastic composites, sizing has a pronounced beneficial effect on interfacial properties [18].

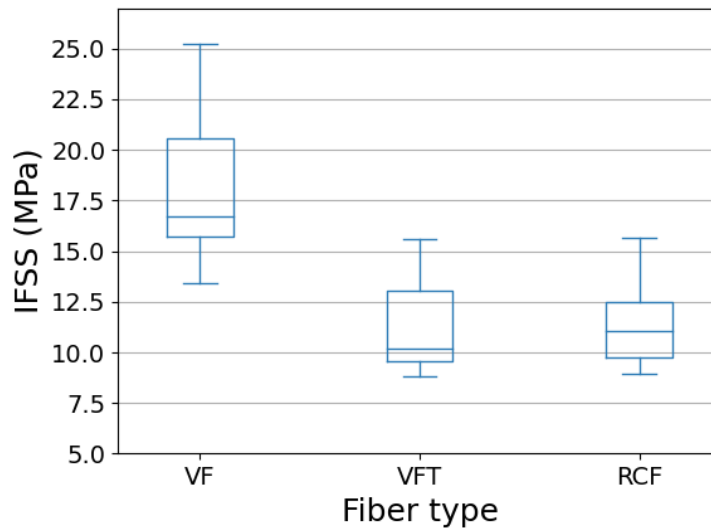


**Figure 7 - IFSS values obtained for each fibre type**

It raises the question of RCF re-sizing or more generally surface treatments. The viability of surface treatments to restore the RCF capacity to adhere to a thermoplastic matrix is a promising path for future research.

## 5 CONCLUSION

The intrinsic mechanical properties of sized (VF), de-sized (VFT), and reclaimed carbon fibres (RCF) were measured and compared. The recovery process was found to have a limited impact on the mechanical properties of the fibres, as a minor 15 % decrease in their tensile strength and an unchanged elastic modulus were observed. RCF are not limited in their reuse by their mechanical properties, but by their degraded surface properties that prevent adhesion to the matrix as well as interfacial properties.

SEM and AFM scans highlight very different surface morphologies between RCF, VFT and VF. The presence of polymeric residues on RCF alongside smooth portions of bare fibre very similar to VFT surface result in a higher mean roughness that could facilitate the adhesion with the matrix. Moreover, RCF present higher values of surface energy compared to VFT that should potentially improve the adhesion with the matrix. In order to explain the different ratios of dispersive versus polar components a finer analysis of the fibre surfaces chemical state could be useful. Although RCF exhibited a higher surface energy than VFT, no significant advantage in cohesion could be observed via IFSS tests.

The results presented in this study contribute to identify the key parameters that influence fibre/matrix interfacial properties at the microscale. Further investigations at the larger scale of composite constitute the perspective of this work. Additionally, surface treatments such as plasma functionalization, re-sizing or chemical oxidation of the surface could be useful to further enhance adhesion between fibres and matrix and thus the mechanical performance of the fibre/matrix interface.

## REFERENCES

- [1] D.R. Vieira, R.K. Vieira, M. Chang Chain, Strategy and management for the recycling of carbon fiber-reinforced polymers (CFRPs) in the aircraft industry: a critical review, *Int. J. Sustain. Dev. World Ecol.* 24 (2017) 214–223.
- [2] T.K. Das, P. Ghosh, N.C. Das, Preparation, development, outcomes, and application versatility of carbon fiber-based polymer composites: a review, *Adv. Compos. Hybrid Mater.* 2 (2019) 214–233.

- [3] F. Meng, J. McKechnie, T. Turner, K.H. Wong, S.J. Pickering, Environmental aspects of use of recycled carbon fiber composites in automotive applications, *Environ. Sci. Technol.* 51 (2017) 12727–12736.
- [4] F. Meng, E.A. Olivetti, Y. Zhao, J.C. Chang, S.J. Pickering, J. McKechnie, Comparing life cycle energy and global warming potential of carbon fiber composite recycling technologies and waste management options, *ACS Sustain. Chem. Eng.* 6 (2018) 9854–9865.
- [5] Y.F. Khalil, Sustainability assessment of solvolysis using supercritical fluids for carbon fiber reinforced polymers waste management, *Sustain. Prod. Consum.* 17 (2019) 74–84.
- [6] F.A. López, O. Rodríguez, F.J. Alguacil, I. García-Díaz, T.A. Centeno, J.L. García-Fierro, C. González, Recovery of carbon fibres by the thermolysis and gasification of waste prepreg, *J. Anal. Appl. Pyrolysis.* 104 (2013) 675–683.
- [7] S.H. Han, H.J. Oh, S.S. Kim, Evaluation of fiber surface treatment on the interfacial behavior of carbon fiber-reinforced polypropylene composites, *Compos. Part B Eng.* 60 (2014) 98–105.
- [8] M. Holmes, Recycled carbon fiber composites become a reality, *Reinf. Plast.* 62 (2018) 148–153.
- [9] M.H. Akonda, C.A. Lawrence, B.M. Weager, Recycled carbon fibre-reinforced polypropylene thermoplastic composites, *Compos. Part Appl. Sci. Manuf.* 43 (2012) 79–86.
- [10] C.D. Volpe, S. Siboni, The Wilhelmy method: a critical and practical review, *Surf. Innov.* 6 (2018) 120–132.
- [11] Y. Ma, C. Yan, H. Xu, D. Liu, P. Shi, Y. Zhu, J. Liu, Enhanced interfacial properties of carbon fiber reinforced polyamide 6 composites by grafting graphene oxide onto fiber surface, *Appl. Surf. Sci.* 452 (2018) 286–298.
- [12] M.B. Villarino, Ramanujan’s inverse elliptic arc approximation, *Ramanujan J.* 34 (2014) 157–161.
- [13] D. He, V.K. Soo, F. Stojcevski, W. Lipiński, L.C. Henderson, P. Compston, M. Doolan, The effect of sizing and surface oxidation on the surface properties and tensile behaviour of recycled carbon fibre: An end-of-life perspective, *Compos. Part Appl. Sci. Manuf.* 138 (2020) 106072.
- [14] J.-S. Jeong, K.-W. Kim, K.-H. An, B.-J. Kim, Fast recovery process of carbon fibers from waste carbon fibers-reinforced thermoset plastics, *J. Environ. Manage.* 247 (2019) 816–821.
- [15] T.R. Abdou, A.B. Junior, D.C.R. Espinosa, J.A.S. Tenório, Recycling of polymeric composites from industrial waste by pyrolysis: Deep evaluation for carbon fibers reuse, *Waste Manag.* 120 (2021) 1–9.
- [16] W. Garat, M.F. Pucci, R. Leger, Q. Govignon, F. Berthet, D. Perrin, P. Jenny, P.-J. Liotier, Surface energy determination of fibres for Liquid Composite Moulding processes: Method to estimate equilibrium contact angles from static and quasi-static data, *Colloids Surf. Physicochem. Eng. Asp.* 611 (2021) 125787.
- [17] X. Chen, H. Xu, D. Liu, C. Yan, Y. Yao, Y. Zhu, Effect of hybrid polysphosphazene coating treatment on carbon fibers on the interfacial properties of CF/PA6 composites, *J. Appl. Polym. Sci.* 137 (2020) 49577.
- [18] R.L. Zhang, Y.D. Huang, D. Su, L. Liu, Y.R. Tang, Influence of sizing molecular weight on the properties of carbon fibers and its composites, *Mater. Des.* 34 (2012) 649–654.